Interphotoreceptor Retinoid-Binding Protein Mitigates Cellular Oxidative Stress and Mitochondrial Dysfunction Induced by All-*trans*-Retinal

Minsup Lee, Songhua Li, Kota Sato,* and Minghao Jin

Department of Ophthalmology and Neuroscience Center, Louisiana State University Health Sciences Center, New Orleans, Louisiana, United States

Correspondence: Minghao Jin, Department of Ophthalmology and Neuroscience Center, LSU Health Sciences Center, New Orleans, LA 70112, USA;
mjin@lsuhsc.edu.

Current affiliation: *Department of Ophthalmology, Tohoku University School of Medicine, Sendai, Japan.

Submitted: October 30, 2015
Accepted: February 29, 2016

Citation: Lee M, Li S, Sato K, Jin M. Interphotoreceptor retinoid-binding protein mitigates cellular oxidative stress and mitochondrial dysfunction induced by all-*trans*-retinal. *Invest Ophthalmol Vis Sci*. 2016;57:1553–1562. DOI:10.1167/iovs.15-18551

Purpose. Point and null mutations in interphotoreceptor retinoid-binding protein (IRBP) cause retinal dystrophy in affected patients and IRBP-deficient mice with unknown mechanism. This study investigated whether IRBP protects cells from damages induced by all-*trans*-retinal (a*t*RAL), which was increased in the *Irbp*$^{-/-}$ retina.

Methods. Wild-type and *Irbp*$^{-/-}$ mice retinal explants in buffer with or without purified IBRP were exposed to 800 lux light for different times and subjected to retinoid analysis by high-performance liquid chromatography. Purity of IRBP was determined by Coomassie Brilliant Blue staining and immunoblot analysis. Cellular damages induced by a*t*RAL in the presence or absence of IRBP were evaluated in the mouse photoreceptor-derived 661W cells. Cell viability and death were measured by 3-(4,5-dimethyl-2-yl)-5-(3-carboxymethoxyphenyl)-2-(4-sulfophenyl)-2H-tetrazolium (MTS) and TUNEL assays. Expression and modification levels of retinal proteins were determined by immunoblot analysis. Intracellular reactive oxygen species (ROS) and nitric oxide (NO) were detected with fluorogenic dyes and confocal microscopy. Mitochondrial membrane potential was analyzed by using JC-1 fluorescent probe and a flow cytometer.

Results. Content of a*t*RAL in *Irbp*$^{-/-}$ retinal explants exposed to light for 40 minutes was significantly higher than that in wild-type retinas under the same light conditions. All-*trans*-retinal caused increase in cell death, tumor necrosis factor activation, and Adam17 upregulation in 661W cells. NADPH oxidase-1 (NOX1) upregulation, ROS generation, NO-mediated protein *S*-nitrosylation, and mitochondrial dysfunction were also observed in 661W cells treated with a*t*RAL. These cytotoxic effects were significantly attenuated in the presence of IRBP.

Conclusions. Interphotoreceptor retinoid-binding protein is required for preventing accumulation of retinal a*t*RAL, which causes inflammation, oxidative stress, and mitochondrial dysfunction of the cells.

Keywords: visual cycle, IRBP, all-*trans*-retinal, retinal degeneration, photoreceptor

The light-sensitive chromophore of the visual pigments in cone and rod photoreceptors is 11-*cis*-retinal (11*c*RAL). It keeps the visual pigments in an inactive conformation and functions as a molecular switch for activating opsins in response to light stimulation. When light hits the visual pigments, its energy converts 11*c*RAL to all-*trans*-retinal (a*t*RAL), inducing structural rearrangement and activation of opsins. The activated opsins then trigger the phototransduction that converts light signal into electrical and neural signals in the photoreceptors. Both 11*c*RAL and a*t*RAL possess a highly reactive aldehyde group and are the precursors of A2E,[1,2] a cytotoxic byproduct of the retinoid visual cycle necessary for regenerating 11*c*RAL.[3] Several studies have suggested that a*t*RAL is a critical pathogenic factor in light-induced retinal degeneration and retinopathy of mouse model.[4] In addition, A2E and a*t*RAL dimer have been suggested to contribute to the pathology of Stargardt disease.[5] These studies indicate that preventing excess accumulation of a*t*RAL and 11*c*RAL is important for maintaining retinal health.

Interphotoreceptor retinoid-binding protein (IRBP) expressed by photoreceptors is known to bind with 11*c*RAL, a*t*RAL, 11-*cis*-retinol (11*c*ROL), and all-*trans*-retinol (a*t*ROL).[6–9] This 140-kDa secretory glycoprotein with four homologous modules is the most abundant soluble protein in the interphotoreceptor matrix (IPM).[10,11] The high abundance implicates its important role in protecting, solubilizing, and detoxifying retinoids in the IPM and photoreceptors. In ex vivo experiments, IRBP has been shown to promote release of 11*c*RAL from the retinal pigment epithelium (RPE)[12,13] and a*t*ROL from the neural retina after photobleaching of the visual pigments.[14–16] *Irbp*$^{-/-}$ mice display severe retinal degeneration and vision impairment.[17–21]

The significance of IRBP function in human retinal health and vision is reflected by the fact that mutations in IRBP are associated with retinal diseases and vision impairment. Recently, two nonsense mutations (Y510X and E1152X) of IRBP have been identified in children with high myopia and retinal dystrophy.[22] In addition, a missense mutation (D1080N)

This work is licensed under a Creative Commons Attribution-NonCommercial-NoDerivatives 4.0 International License.

has been found in adults with retinitis pigmentosa (RP).[23] The RP-associated missense mutation has been shown to abolish secretion of IRBP in culture cells, suggesting that the mutation results in loss of IRBP in the patients' IPM.[24] Optical coherence tomography and electroretinography have shown that all affected patients with any of the mutations exhibit abnormal retinal structure and severe impairment of both cone and rod visual function,[22,23] suggesting that IRBP is required for normal retinal development or for maintaining retinal structure and function.

We recently have shown that tumor necrosis factor-α (TNF-α), a potent proinflammatory cytokine that can induce cellular apoptosis and necrosis, is increased several-fold in the *Irbp*$^{-/-}$ retina and IPM.[25] However, the molecular mechanisms leading to upregulation and activation of TNF in *Irbp*$^{-/-}$ retina remain unknown. In this study, we first investigated the effect of IRBP deficiency on accumulation of a*t*RAL in the retina. We then analyzed the pathologic roles of a*t*RAL in induction of TNF activation, oxidative stress, mitochondrial dysfunction, and cell death. At the same time, we also investigated protective role of IRBP against a*t*RAL-induced cytotoxicity in the mouse photoreceptor-derived 661W cells.

Methods

Animals and Ex Vivo Experiments

Wild-type (WT) 129S2/Sv (Charles River Laboratories, Wilmington, MA, USA) and *Irbp*$^{-/-}$ mice were maintained in 12-hour cyclic light at ~30 lux. The *Irbp*$^{-/-}$ mice were originally generated by Liou et al.[17] In this study, we used *Irbp*$^{-/-}$ mice with the 129S2/Sv genetic background.[18] All animal experiments followed the ARVO Statement for the Use of Animals in Ophthalmic and Vision Research and the protocols were approved by the Institutional Animal Care and Use Committee. For retinal ex vivo experiments, we isolated retinas from 5-week-old dark-adapted WT and *Irbp*$^{-/-}$ mice and placed each in 100 μL serum-free Dulbecco's modified Eagle's medium (DMEM) (Invitrogen, Carlsbad, CA, USA) containing 20 mM HEPES buffer (pH 7.4). We added 4 μM purified IRBP, which is similar to IRBP concentration in rat IPM,[26] into the media of WT retinal explants. After exposure to white light at 800 lux for 10, 20, or 40 minutes, retinoids were analyzed as described below.

High-Performance Liquid Chromatography Analysis of Retinoids

We converted a*t*RAL and 11*c*RAL to *syn*- and *anti*-retinaloxime isomers by using 150 mM hydroxylamine before extraction of retinoids from retinas.[18] Retinoids were extracted with hexane and analyzed by normal-phase HPLC as previously described.[27] In brief, retinoids in hexane extractions were evaporated, redissolved in 100 μL hexane, and separated on a silica column (Zorbax-Sil 5 μm, 250 × 4.6 mm; Agilent Technologies, Santa Clara, CA, USA) by gradient (0.2%–10% dioxane in hexane at 2.0 mL/min flow rate) elution of mobile phase in an Agilent 1100 HPLC system.

Expression and Purification of IRBP

The 293T-LC cells[28] grown in DMEM containing 10% fetal bovine serum (FBS) were transfected with IRBP-expression plasmid (pIRBP)[18] or pRK5 mock vector, as described previously.[29] One day after transfection, we replaced the media with fresh serum-free or 1% FBS-containing DMEM and incubated an additional 16 hours. The media were centrifuged at 20,000*g* for 30 minutes. Presence of IRBP in the serum-free media of the pIRBP-transfected (IRBP-medium) or pRK5-transfected (mock-medium) cells was analyzed by Coomassie Brilliant Blue (CBB) staining and immunoblot analysis using an antibody against IRBP.[24] The IRBP-medium and mock-medium were then concentrated with Amicon Ultra 100-KD molecular-weight cutoff (Millipore, Billerica, MA, USA). To purify IRBP from the 1% FBS-containing media, we precipitated IRBP with 16% saturated ammonium sulfate. The precipitates were resolved in 50 mM Tris-HCl buffer (pH 7.5) containing EDTA-free protease inhibitors, 150 mM NaCl, and 0.1 mM dithiothreitol, and were incubated with concavalin A (ConA) Sepharose 4B (GE Healthcare, Pittsburgh, PA, USA). After washing three times, IRBP was eluted with the buffer containing 10% methyl a-D-mannopyranoside (Sigma-Aldrich Corp., St. Louis, MO, USA). Purity of IRBP was analyzed by CBB staining and immunoblot analysis.

Cell Viability Assay

The 661W cells, a mouse photoreceptor-derived cell line, were kindly provided by Muayyad R. Al-Ubaidi at the University of Oklahoma and were maintained as described previously.[30] For cell viability assay, the cells at a density of 3×10^3 cells/well in a 96-well plate were incubated with the indicated concentration of a*t*RAL in serum-free medium with or without IRBP for 24 hours. Cell viability was determined by using a CellTiter^{96} AQueous assay kit (Promega, Madison, WI, USA) as described previously.[31] Briefly, the culture media were replaced with 95 μL fresh media containing 5 μL 3-(4,5-dimethyl-2-yl)-5-(3-carboxymethoxyphenyl)-2-(4-sulfophenyl)-2H-tetrazolium (MTS) solution. After 1 hour, the absorbance at 490 nm was measured by using a microplate reader (Molecular Device, Sunnyvale, CA, USA).

TUNEL Assay

Detection and quantification of cell death at single-cell level was determined by TUNEL assay using the in situ cell death detection kit (Roche, Indianapolis, IN, USA), according to the manufacturer's protocol. Briefly, 661W cells on glass coverslips (5×10^5 cells/well in six-well plate) were treated with 1.8 μM a*t*RAL, washed with phosphate-buffered saline (PBS), fixed with 4.0% paraformaldehyde in PBS for 15 minutes, and then permeabilized with 0.5% Triton X-100 in PBS for 10 minutes. After incubation with the mixture of enzyme solution and label solution for 1 hour at 37°C, fluorescent signals were captured with a Zeiss LSM710 Meta confocal microscope (Oberkochen, Germany) with an ×20 objective lens.

Measurement of Intracellular Reactive Oxygen Species (ROS) and Nitric Oxide (NO)

The cellular ROS and NO were measured by using 2′,7′-dichlorodihydrofluorescein diacetate (DCFH-DA) (Sigma-Aldrich Corp.) and 4,5-diaminofluorescein diacetate (DAF-2DA) (Sigma-Aldrich Corp.), respectively. 661W cells in a Corning Costar 96-well black clear-bottom plate at a density of 3×10^3 cells/well were incubated with 1.8 μM a*t*RAL in the presence or absence of IRBP for 2 hours, and then with 20 μM DCFH-DA or 10 μM DAF-2DA for 20 minutes. After washing with PBS twice, the relative fluorescence unit was measured at an excitation wavelength of 485 nm and an emission wavelength of 528 nm with a fluorescence microplate reader (Molecular Device). The cells incubated in the same condition were used for capturing fluorescent signals with a Zeiss LSM710 Meta confocal microscope with an ×20 objective lens. Each image

Investigative Ophthalmology & Visual Science

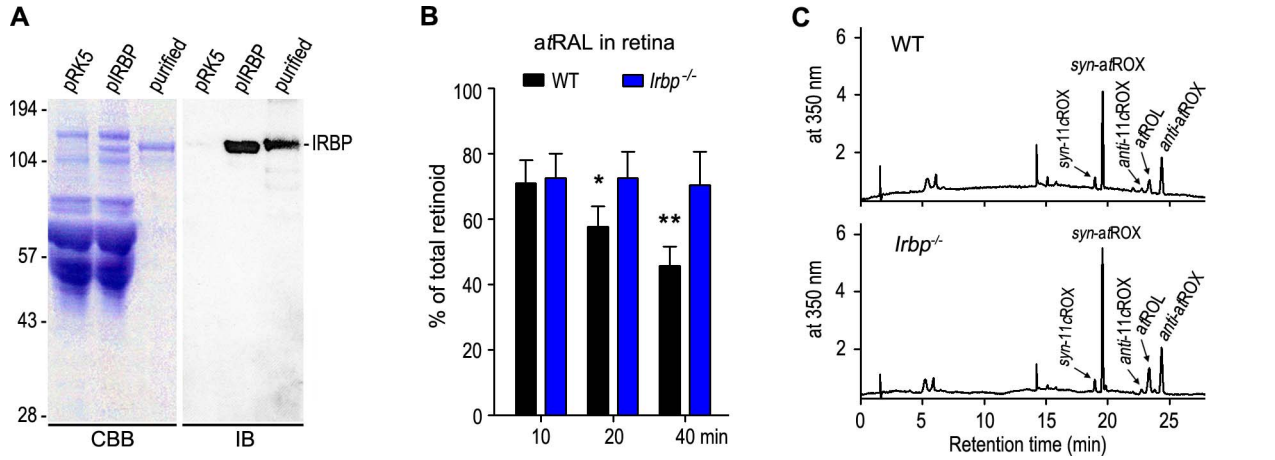

Figure 1. Interphotoreceptor retinoid-binding protein is required for reducing *at*RAL in retina exposed to light. (**A**) Media of 293T-LC cells transfected with pRK5 or pIRBP and IRBP purified from the pIRBP-transfected cell medium were analyzed by CBB staining and immunoblot (IB) analysis. (**B**) Relative contents of *at*RAL in WT and *Irbp*$^{-/-}$ mice retinal explants exposed to 800 lux light for the indicated times. Wild-type and *Irbp*$^{-/-}$ retinal explants were incubated in buffer with or without purified IRBP, respectively. *Asterisks* indicate significant differences between WT and *Irbp*$^{-/-}$ mice (*$P < 0.05$, **$P < 0.01$). *Error bars* indicate SD ($n = 4$). (**C**) Representative HPLC chromatograms of retinoids in WT and *Irbp*$^{-/-}$ retinas exposed to 800 lux light for 40 minutes. The peaks of *at*ROL, *syn*- and *anti*-retinaloxime (ROX) isomers of 11*c*RAL and *at*RAL are labeled.

was collected under the same system settings (e.g., the same laser intensity and scan speed).

Preparation of Cell Lysates and Mitochondrial and Nuclear Fractions

661W cells incubated with *at*RAL in serum-free media with or without IRBP were washed with ice-cold PBS containing protease and phosphatase inhibitors and incubated with lysis buffer (50 mM Tris-HCl, 150 mM NaCl, 1% Triton X-100, 1% SDS, 1% Nonidet P-40, 1 mM EDTA, 1 mM dithiothreitol, 200 nM aprotinin, 20 μM leupetin, 50 μM phenanthroline, 280 μM benzamidine-HCl) for 30 minutes on ice. After centrifugation at 16,000*g* for 20 minutes at 4°C, the supernatant was used as the cell lysates. Mitochondrial and nuclear fractions were prepared from 661W cells by using the Cell Fractionation Kit (Abcam, Cambridge, MA, USA), according to the manufacturer's protocol.

Analysis of Mitochondrial Membrane Potentials

661W cells were incubated with 1.8 μM *at*RAL in fresh serum-free medium, in IRBP-medium, or in mock-medium for 6 hours. After washing with PBS, the cells were incubated with 2.5 μg/mL 5,5′,6,6′-tetrachloro-1,1,3′,3′-tetraethylbenzimidazolylcarbocyanine iodide (JC-1) (Thermo Fisher Scientific, Waltham, MA, USA) for 20 minutes. JC-1 is a green fluorescent cationic carbocyanine dye that enters the negatively charged mitochondrial matrix and forms J-aggregates that exhibit red fluorescence. After washing with PBS, the green fluorescent JC-1 monomers and the red fluorescent J-aggregates in the cells were detected with a Gallios Flow Cytometer (Beckman Coulter, Brea, CA, USA). A total of 30,000 cells were acquired. The data were analyzed by using the Kaluza Analysis Software and displayed in histogram of JC-1 green fluorescence and in dot plot of J-aggregate red fluorescence (*y*-axis) against JC-1 green fluorescence (*x*-axis).

Immunoblot Analysis

Proteins were separated in an 8%, 10%, or 12% polyacrylamide gel by sodium dodecyl sulfate–polyacrylamide gel electrophoresis, and transferred onto an Immobilon-P membrane (Millipore). The membrane was incubated sequentially in blocking buffer, primary antibody, and horseradish peroxidase–conjugated anti-mouse or rabbit IgG secondary antibody. Antibodies against β-actin (Sigma-Aldrich Corp.), IRBP,[24] TNF (Abcam), Adam17 (Chemicon, Billerica, MA, USA), *S*-nitrosocysteine (Sigma-Aldrich Corp.), apoptosis inducing factor (AIF) (Abcam), NADPH oxidase-1 (NOX1; GeneTex, Irvine, CA, USA), and PARP1 (Cell Signaling Technology, Danvers, MA, USA) were used as the primary antibodies. Immunoblots were visualized and quantified as described.[32]

Statistical Analysis

Data were expressed as means ± standard deviation (SD) from at least three separate experiments unless otherwise indicated. Data were analyzed by using 1-way analysis of variance, followed by each pair of Student's *t*-tests for multiple comparisons. All analyses were done with Microsoft Excel software (Microsoft, Redmond, WA, USA).

Results

Accumulation of *at*RAL in *Irbp*$^{-/-}$ Retina Exposed to Light

Since IRBP has been shown to play an important role in protection and transportation of retinoids, we tested if *at*RAL accumulates in *Irbp*$^{-/-}$ retina after long-time photobleaching of the visual pigments. To do this experiment, we purified IRBP from pIRBP-transfected 293T-LC cell media by a ConA affinity chromatography (Fig. 1A). We then placed dark-adapted WT and *Irbp*$^{-/-}$ retinas in IRBP-containing or not containing buffer, which mimics WT and *Irbp*$^{-/-}$ IPMs, respectively. After exposure to bright light for different times, we analyzed retinoids in the retinas. Since *Irbp*$^{-/-}$ mice had retinal degeneration, we expressed the levels of *at*RAL as the percentage of total retinoids. As shown in Figure 1B, *at*RAL in WT retina decreased as light-exposure time increased. The amounts of *at*RAL in WT retina exposed to light for 40 minutes was significantly lower than those in WT retina exposed to light for 10 minutes ($P < 0.01$). However, the amounts of *at*RAL in *Irbp*$^{-/-}$ retina were not greatly changed during 10 to 40

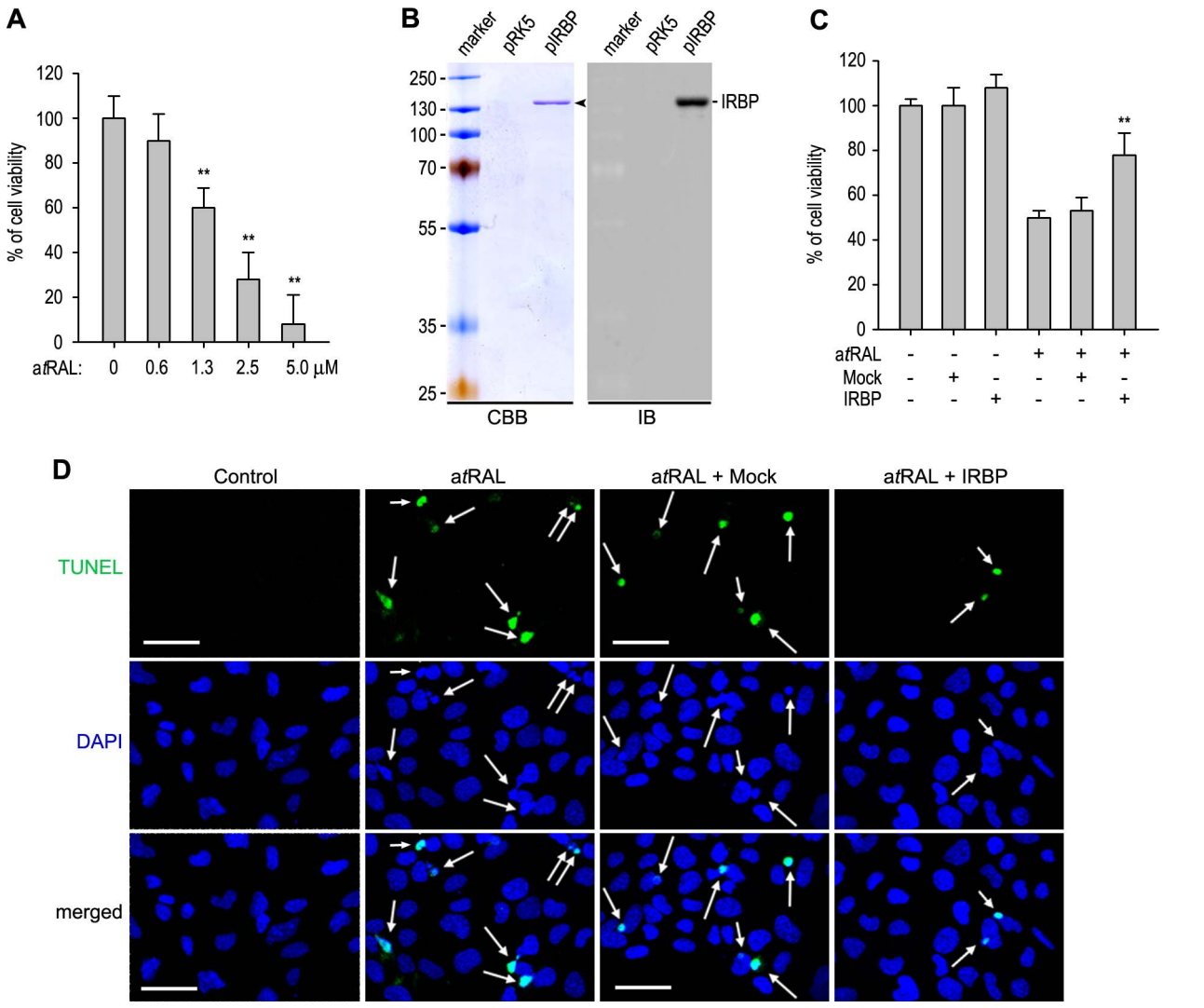

Figure 2. Interphotoreceptor retinoid-binding protein alleviated cell death induced by atRAL. (**A**) Viabilities of 661W cells incubated with the indicated concentration of atRAL in serum-free medium were determined by MTS assay. $^{**}P < 0.01$ indicates significant differences between control and atRAL-treated cells. (**B**) Coomassie Brilliant Blue staining and IB analysis of IRBP in serum-free media of 293T-LC cells transfected with pRK5 or pIRBP. (**C**) Viabilities of 661W cells incubated with 0 or 1.8 μM atRAL in fresh medium or medium of 293T-LC cells transfected with pRK5 (mock) or pIRBP (IRBP). (**D**) TUNEL assay of 661W cells incubated with 1.8 μM atRAL as in (**C**). Nuclei were counterstained with 4′,6-diamidino-2-phenylindole (DAPI). TUNEL-positive nuclei were indicated with *arrows*. *Scale bars*: 50 μm.

minutes of light-exposure time (Fig. 1B). As a result, the contents of atRAL in *Irbp*$^{-/-}$ retina exposed to light for longer times were significantly higher than those in WT retina (Figs. 1B, 1C).

IRBP Alleviated Cell Death Induced by atRAL

Since atRAL possesses a highly reactive aldehyde group, we tested the effects of atRAL on cell viability. We incubated 661W cells with a series of increasing concentration (0–5 μM) of atRAL for 24 hours. As shown in Figure 2A, cell viability was significantly decreased by atRAL treatment in a dose-dependent manner. The estimated IC_{50} was approximately 1.8 μM. To examine the effect of IRBP on the atRAL-mediated inhibition of cell viability, we performed the cell viability assay with 1.8 μM atRAL in the IRBP-medium or mock-medium. Coomassie Brilliant Blue and immunoblot staining revealed that the IRBP-medium, but not the mock-medium, contained relatively pure IRBP (Fig. 2B). Cell viability assay showed that viabilities of 661W cells incubated with atRAL in the mock-medium were similar to those of cells incubated with atRAL in fresh serum-free medium (Fig. 2C). In contrast, the viabilities of the cells incubated with atRAL in the IRBP-medium were increased by at least 25% (Fig. 2C). Consistent with these results, the number of TUNEL-positive nuclei was significantly reduced in the cells incubated with atRAL in the IRBP-medium, as compared to the cells incubated with atRAL in the mock-medium (Fig. 2D).

IRBP Attenuated TNF Activation Triggered by atRAL

In a previous study,[25] we have shown that TNF is dramatically increased in soluble fraction of the *Irbp*$^{-/-}$ IPM. We therefore tested whether atRAL can promote production of soluble TNF (sTNF), the active form of TNF,[33] in 661W cells. We incubated the cells with a series of increasing concentration of atRAL in serum-free media. Immunoblot analysis showed that the cleaved sTNF was increased in a dose-dependent manner (Fig. 3A). The immunoblot intensity of sTNF in the cells treated with 1.8 μM atRAL was approximately 2-fold of that in control cells (Fig. 3A). To test if IRBP inhibits the atRAL-mediated

Investigative Ophthalmology & Visual Science

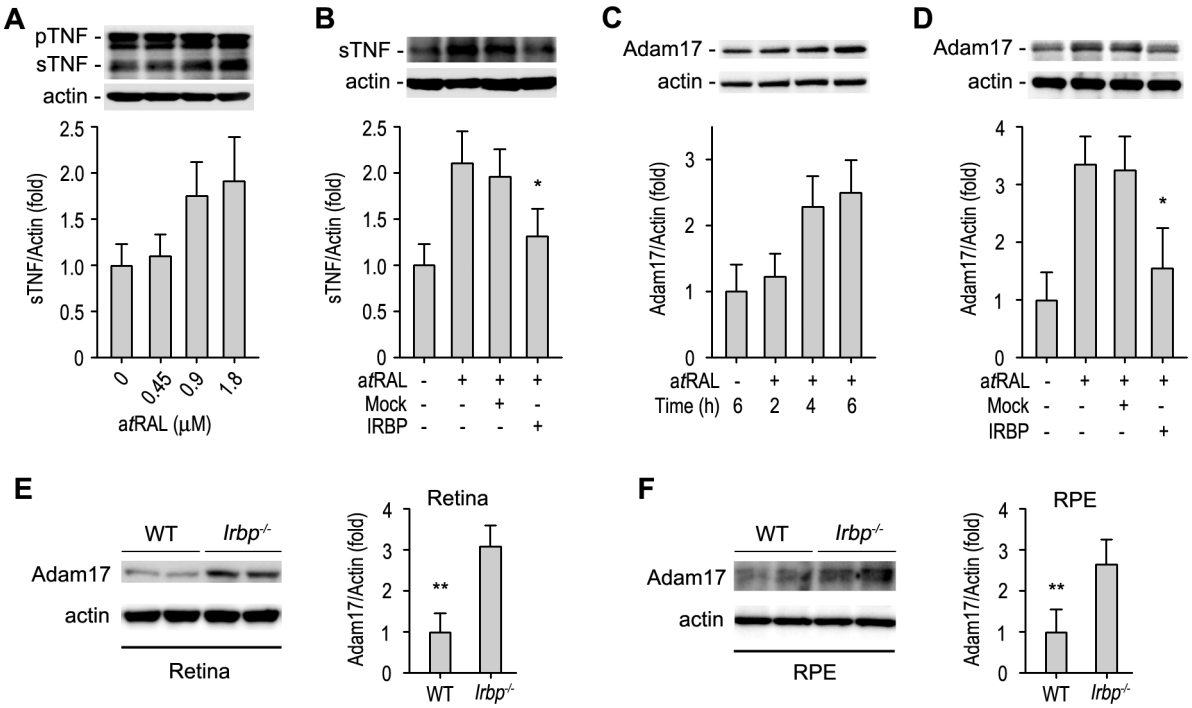

Figure 3. Interphotoreceptor retinoid-binding protein attenuated TNF activation triggered by atRAL. (**A**) Immunoblot analysis showing increase of sTNF in 661W cells treated with atRAL for 6 hours. Histogram shows relative immunoblot intensities of sTNF normalized by actin. (**B**) Immunoblot analysis of sTNF in 661W cells treated with atRAL in serum-free medium, mock-medium, or IRBP-medium. Histogram shows relative immunoblot intensities of sTNF. $^{*}P < 0.05$ indicates significant differences between cells treated with atRAL in mock- versus IRBP-medium. (**C**) Immunoblot analysis of Adam17 in 661W cells treated with atRAL for indicated times. Histogram shows normalized intensities of Adam17 immunoblots. (**D**) Immunoblot analysis of Adam17 in 661W cells treated with atRAL in the indicated media. (**E**, **F**) Immunoblot analysis of Adam17 in the retina (**E**) and RPE (**F**) of WT and *Irbp*$^{-/-}$ mice. $^{**}P < 0.01$ indicates significant differences between WT and *Irbp*$^{-/-}$ tissues. *Error bars* denote SD ($n = 3$).

activation of TNF, we incubated 661W cells with 1.8 μM atRAL either in fresh serum-free medium, IRBP-medium, or mock-medium. As shown in Figure 3B, the atRAL-mediated elevation of sTNF was markedly suppressed by IRBP-medium, but not by mock-medium.

IRBP Inhibited Adam17 Upregulation Induced by atRAL

Since TNF-α converting enzyme (TACE)/Adam17 metalloprotease has been shown to mediate cleavage of membrane-bound pro-TNF in the post-Golgi,[34] we tested the effect of atRAL on expression levels of Adam17 in 661W cells. Immunoblot analysis showed that protein levels of Adam17 (approximately 100 kDa) were increased 50% in the cells treated with 1.8 μM atRAL for 4 to 6 hours (Fig. 3C). This upregulation of Adam17 was significantly attenuated by incubation of atRAL with IRBP-medium (Fig. 3D). To test if Adam17 is upregulated in the *Irbp*$^{-/-}$ retina and RPE, we compared expression levels of Adam17 in WT and *Irbp*$^{-/-}$ tissues. Immunoblot analysis showed that Adam17 was increased at least 2-fold in the *Irbp*$^{-/-}$ retina and RPE (Figs. 3E, 3F).

IRBP Suppressed atRAL-Induced Production of ROS in 661W Cells

To analyze the mechanism by which atRAL causes cell damage, we tested if atRAL stimulates ROS generation in 661W cells. DCFH-DA is a cell-permeable fluorogenic probe. Reactive oxygen species in the cells convert DCFH-DA to highly fluorescent DCF. We incubated DCFH-DA with 661W cells treated with 0 to 1.8 μM atRAL in the presence or absence of IRBP. Confocal microscopy showed that the DCF fluorescent signal was dramatically increased in the cells treated with atRAL in fresh medium, as compared to the control cells maintained in fresh medium without atRAL (Figs. 4A, 4B). The DCF fluorescent signal was significantly decreased in the cells treated with atRAL in the IRBP-medium, but not in the mock-medium (Figs. 4A, 4B). We then analyzed expression of NOX1, a catalytic subunit of the superoxide-generating NADPH oxidase, in 661W cells. Immunoblot analysis showed that atRAL stimulated expression of NOX1 in a time-dependent manner (Fig. 4C). To test if IRBP suppresses the atRAL-induced upregulation of NOX1, we incubated 661W cells with atRAL in the IRBP-medium or mock-medium. Immunoblot analysis showed that the IRBP-medium, but not mock-medium, significantly reduced expression levels of NOX1 in the cells (Fig. 4D). To confirm this result in vivo, we analyzed expression levels of NOX1 in the retina and RPE of WT and *Irbp*$^{-/-}$ mice. As shown in Figures 4E and 4F, NOX1 was increased more than 2-fold in the *Irbp*$^{-/-}$ retina and RPE compared to WT retina and RPE.

IRBP Attenuated atRAL-Induced Production of NO

Since NO also plays an important role in induction of oxidative condition,[35] we tested if atRAL increases intracellular NO level in 661W cells. To detect NO we used DAF-2DA, a fluorescent detector of NO in living cells. Confocal pictures showed that the fluorescent signal (red) of DAF in 661W cells treated with 1.8 μM atRAL in fresh medium was drastically increased as compared to the control cell maintained in fresh medium without atRAL (Figs. 5A, 5B). The IRBP-containing medium, but not mock-medium, significantly attenuated NO production stimulated by atRAL (Figs. 5A, 5B). To confirm these results, we analyzed the levels of protein nitration in the cells. Immuno-

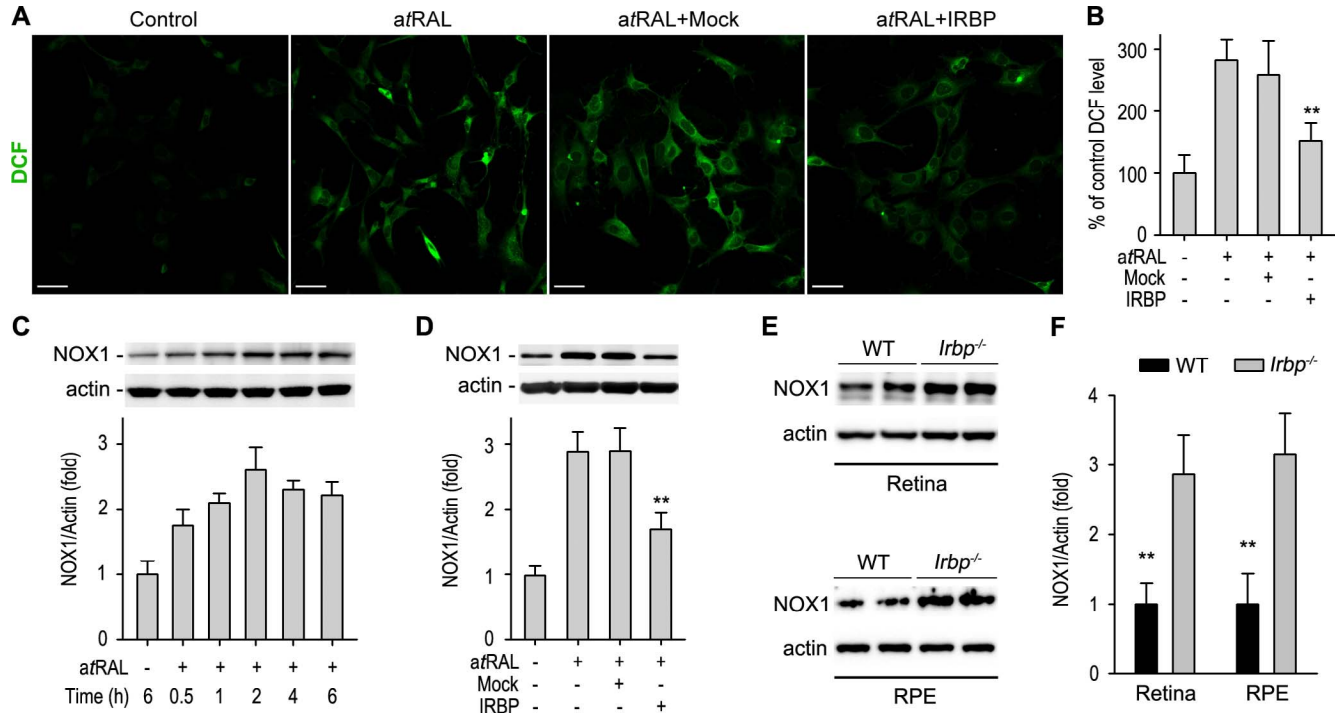

Figure 4. Interphotoreceptor retinoid-binding protein suppressed *at*RAL-induced production of ROS. (**A**) Cells treated with a*t*RAL in fresh serum-free, mock-, or IRBP-medium were incubated with the DCFH-DA fluorogenic probe. Reactive oxygen species–induced fluorescence was visualized by confocal microscopy. *Scale bars*: 50 μm. (**B**) Relative fluorescence intensities in the cells shown in (**A**). Similar results were observed in three independent experiments. $^{**}P < 0.01$ indicates significant differences between cells treated with a*t*RAL in mock- versus IRBP-medium. (**C**) Immunoblot analysis showing increase of NOX1 in the cells treated with a*t*RAL for indicated times. Histogram shows relative intensities of NOX1 immunoblots normalized by actin. *Error bars* denote SD ($n = 3$). (**D**) Immunoblot analysis of NOX1 in 661W cells treated with a*t*RAL either in serum-free, mock-, or IRBP-medium for 2 hours. Normalized intensities of NOX1 immunoblots are shown in the histogram. (**E, F**) Immunoblot analysis (**E**) and relative immunoblot intensities (**F**) of NOX1 in the retina and RPE of WT and *Irbp*$^{-/-}$ mice. $^{**}P < 0.01$ indicates significant differences between WT and *Irbp*$^{-/-}$ tissues.

blot analysis using an antibody against *S*-nitrosocysteine showed that a*t*RAL treatment promoted protein nitration in a time-dependent manner (Figs. 5C, 5D). This a*t*RAL-induced protein nitration was significantly attenuated by the IRBP-medium, but not by mock-medium (Figs. 5E, 5F).

IRBP Mitigated Mitochondrial Dysfunction Induced by a*t*RAL

Oxidative stress has been shown to cause mitochondrial dysfunction.[36] We therefore analyzed mitochondrial membrane potentials by using a cell-permeable JC-1 dye, a mitochondrial potential indicator that exists either as a green fluorescent monomer at depolarized membrane potentials or as a red fluorescent J-aggregate at hyperpolarized membrane potentials. As shown in Figures 6A and 6B, the populations of cells with green fluorescence were increased in the cells treated with a*t*RAL in fresh medium (20% ± 1.2%) or mock-medium (23% ± 1.0%), as compared to the untreated control cells (3.9% ± 0.1%) or the cells treated with a*t*RAL in IRBP-medium (4.6% ± 0.8%).

We then further analyzed the mitochondrial integrity by detecting AIF in mitochondrial and nuclear fractions. Apoptosis inducing factor is normally localized to mitochondria, but when mitochondrion is damaged, it moves to the cytosol and the nucleus.[37] Quantitative immunoblot analysis showed that AIF was increased in the nuclear fraction of 661W cells treated with a*t*RAL in fresh medium or mock-medium, as compared to the control cells and the cells treated with a*t*RAL in IRBP-medium (Figs. 6C, 6D). In contrast, AIF was decreased in the mitochondrial fraction of 661W cells treated with a*t*RAL in fresh medium or mock-medium, as compared to the control cells and the cells treated with a*t*RAL in IRBP-medium (Figs. 6C, 6E).

Discussion

Using purified IRBP and retinal explants of WT and *Irbp*$^{-/-}$ mice, we demonstrated that IRBP is essential for preventing accumulation of a*t*RAL in the retina under bright light conditions. Furthermore, we found that IRBP plays an important role in protection of the mouse photoreceptor-derived 661W cells from TNF activation, oxidative stress, and mitochondrial dysfunction caused by a*t*RAL. These findings may reflect a mechanism of IRBP function in retinal neuroprotection.

The well-known biochemical function of IRBP is its high-affinity binding with retinoids involved in the visual cycle. Although all retinoid isomers can bind with IRBP, the major composition of retinoids bound to IRBP changes depending on light condition. In dark-adapted eyes, 11*c*RAL increases while a*t*ROL decreases. In light-exposed eyes, however, a*t*ROL and a*t*RAL increases, whereas 11*c*RAL decreases.[7,8] Retinols decompose rapidly into a number of products, including their aldehyde form, retinals.[9] Interphotoreceptor retinoid-binding protein has been shown to protect retinol from isomerization, oxidation, and photodegradation.[9,38] In this study, we observed that the content of a*t*RAL in *Irbp*$^{-/-}$ retinal explants exposed to light for 40 minutes was significantly higher than that in WT retinas under the same light conditions (Fig. 1). Since IRBP

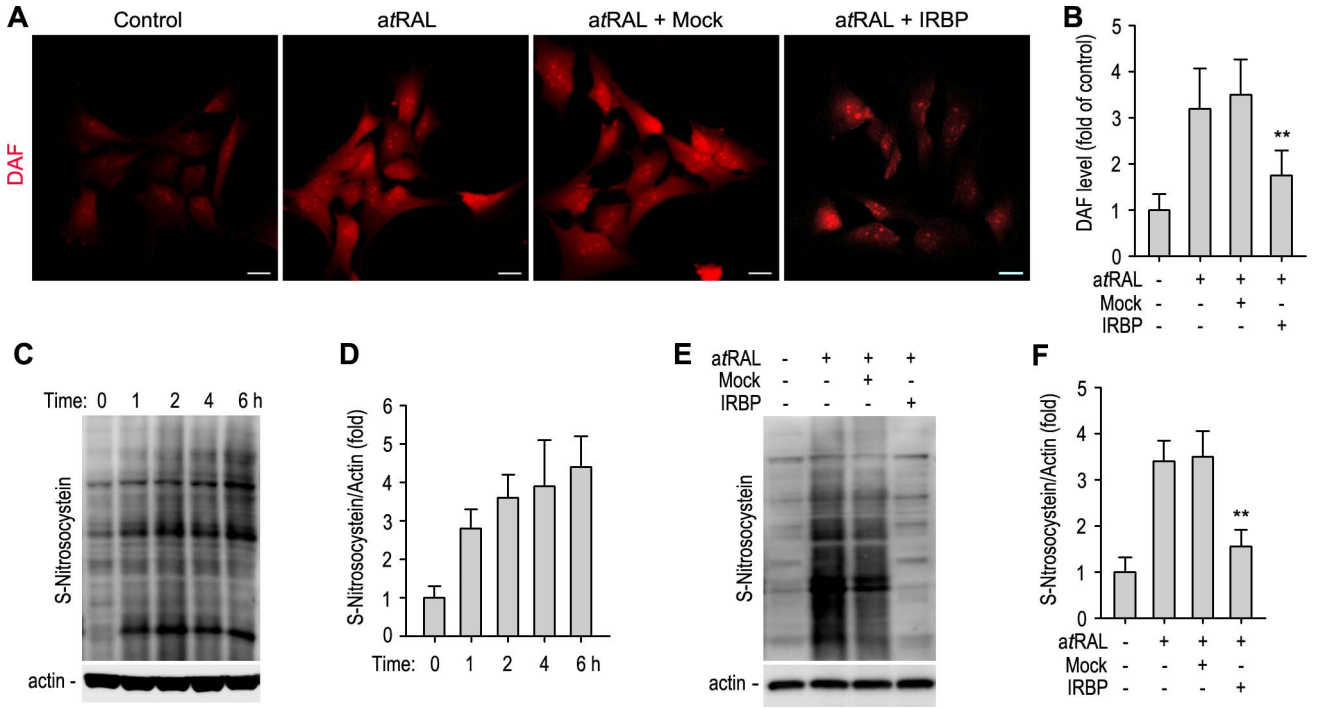

Figure 5. Interphotoreceptor retinoid-binding protein attenuated a*t*RAL-induced production of NO in 661W cells. (**A**) Cells treated with a*t*RAL in fresh serum-free, mock-, or IRBP-medium were incubated with DAF-2DA fluorescence detector of NO for 20 minutes. Nitric oxide was visualized by confocal microscopy. *Scale bars*: 20 μm. (**B**) Relative DAF intensities in the cells shown in (**A**). Similar results were observed in three independent experiments. $^{**}P < 0.01$ indicates significant differences between cells treated with a*t*RAL in mock- versus IRBP-medium. (**C**) *S*-nitrosylated proteins in the cells treated with a*t*RAL for indicated times were detected by immunoblot analysis with an antibody against *S*-nitrosocysteine. (**D**) Normalized relative immunoblot intensities of *S*-nitrosylated proteins shown in (**C**). (**E**) Immunoblot analysis of *S*-nitrosylated proteins in the cells treated with a*t*RAL in serum-free, mock-, or IRBP-medium. (**F**) Relative immunoblot intensities of *S*-nitrosylated proteins shown in (**E**). $^{**}P < 0.01$ indicates significant differences between cells treated with a*t*RAL in mock- versus IRBP-medium.

promotes the release of a*t*ROL from isolated retina after photobleaching of the visual pigments,[14,15] the higher content of a*t*RAL in the *Irbp*$^{-/-}$ retina could be due to oxidation of a*t*ROL retained in photoreceptors by retinol dehydrogenases (RDHs) and/or by photothermal oxidation.

The neural retina and RPE contain a large amount of retinoids. In dark-adapted eye, at least 80% of total retinoids are 11*c*RAL and localized to the neural retina,[18] mainly in photoreceptors. Following exposure to bright light, which causes large photobleaching of the visual pigments, at least 60% of total retinoids in the neural retina are a*t*RAL.[18] Mutations in retinol dehydrogenase 12 (RDH12), an a*t*RAL reductase in rods and cones,[39] are associated with Leber's congenital amaurosis.[40] Disruption of a*t*RAL clearance pathways in photoreceptors induces severe photoreceptor dystrophy in *Rdh8*$^{-/-}$*Abca4*$^{-/-}$ mice,[4] suggesting that a*t*RAL contributes at least in part to the pathogenic mechanisms of the diseases. In agreement with these studies, we observed that a*t*RAL inhibited cell viability and induced cell death in cultured 661W cells (Fig. 2). We also found that IRBP significantly alleviated cell death induced by a*t*RAL (Fig. 2). The bovine IRBP binds a*t*RAL with approximately 2 μM of K_D and 3.2 of stoichiometry.[41] Structural studies have identified a restrictive hydrophobic cavity and a shallow hydrophobic cleft as ligand-binding sites in the *Xenopus* IRBP.[42,43] These findings suggest that IRBP could prevent direct interaction of a*t*RAL with molecules important for cellular functions by holding a*t*RAL in the cavity and cleft.

Lack of IRBP has been shown to result in increase of TNF in the *Irbp*$^{-/-}$ retina.[25] Tumor necrosis factor is a proinflammatory cytokine that promotes cell death.[44] Tumor necrosis factor mRNA in the *Irbp*$^{-/-}$ retina is 2-fold higher than that in WT retina, whereas the amount of TNF in the *Irbp*$^{-/-}$ IPM is more than 10-fold higher than that in WT IPM,[25] suggesting that secreted sTNF is increased in the *Irbp*$^{-/-}$ IPM. It is known that the secreted sTNF, the more active form of TNF, is derived from the transmembrane-anchored TNF precursor through the TACE/Adam17-mediated proteolytic process in the post-Golgi and plasma membrane.[34,45] In this study, we observed that Adam17 was upregulated in 661W cells by a*t*RAL treatment (Fig. 3C). Consistent with this result, sTNF, but not TNF precursor, was significantly increased in a*t*RAL-treated 661W cells (Fig. 3A). Both sTNF and Adam17 were reduced when the cells were treated with a*t*RAL in the presence of IRBP (Figs. 3B, 3D). These results suggest that a*t*RAL is one of the pathogenic factors that induced upregulation of TNF and Adam17 in the *Irbp*$^{-/-}$ retina and RPE (Figs. 3E, 3F) and that Adam17 upregulated by a*t*RAL promoted secretion of sTNF into the *Irbp*$^{-/-}$ IPM.

Reactive oxygen species and NO are important intracellular messengers that regulate cellular function, survival, and differentiation.[46,47] Reactive oxygen species induce upregulation of Adam17,[48] and NO activates Adam17.[49] We found that a*t*RAL stimulated the generation of ROS and NO in 661W cells (Figs. 4A, 4B, 5A, 5B). These observations suggest that ROS and NO are involved in upregulation and activation of Adam17 in 661W cells treated with a*t*RAL.

Excessive generation of ROS and/or NO induces cellular oxidative and nitrosative stresses by damaging macromolecules important for cellular structure, function, and survival.[35,47] NOX1 plays a critical role in generation of ROS. Reaction between superoxide and NO produces peroxynitrite, a strong oxidant that also causes cellular damage by reacting directly with macromolecules.[35,50] In the present study, we observed

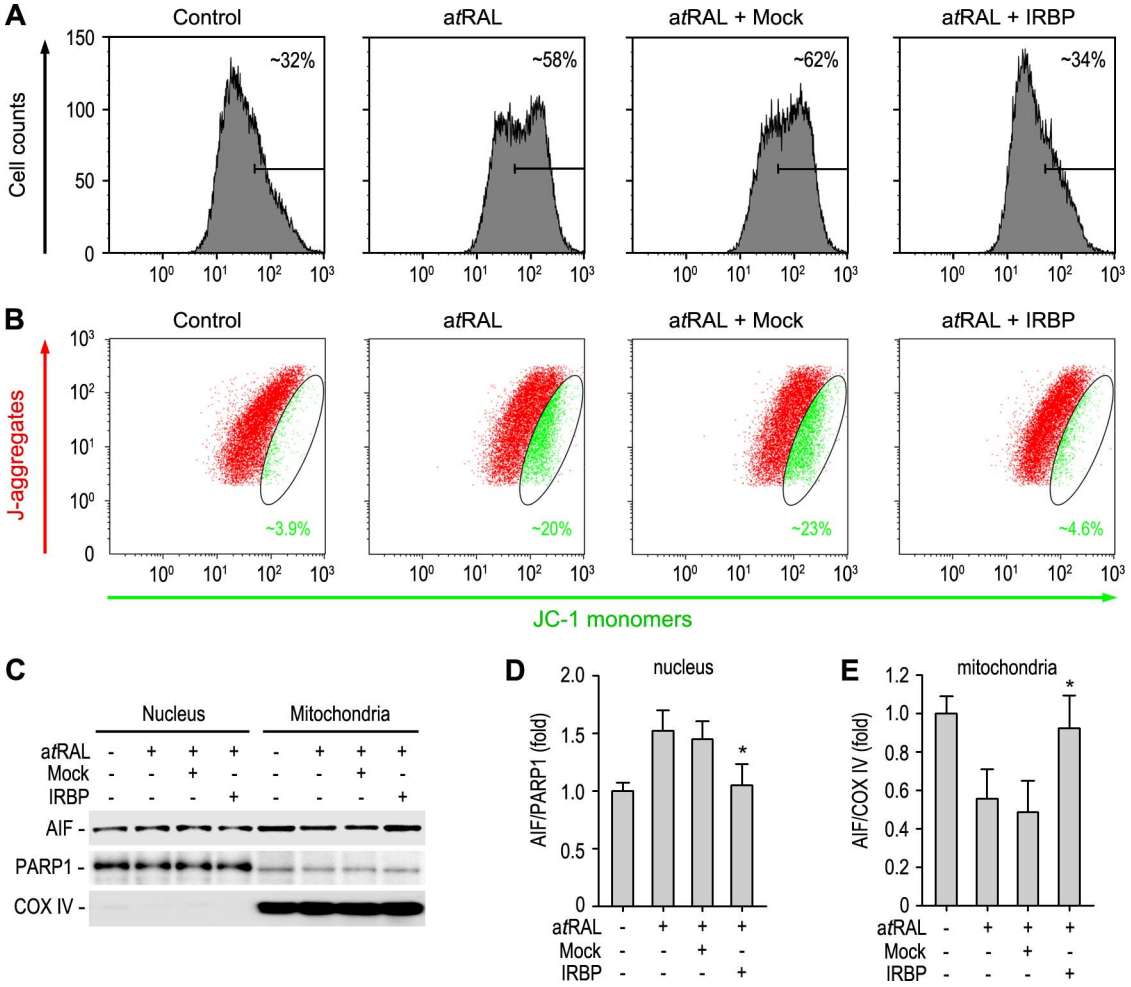

Figure 6. Interphotoreceptor retinoid-binding protein mitigated *at*RAL-induced mitochondrial dysfunction in 661W cells. (**A**, **B**) Cells maintained either in fresh serum-free, mock-, or IRBP-medium containing 1.8 μM *at*RAL were incubated with JC-1 for 20 minutes. Fluorescence density of JC-1 monomers (*x*-axis) was displayed in histogram (**A**), and fluorescence density of J-aggregates (*y*-axis) against JC-1 monomers (*x*-axis) was displayed in dot plot (**B**). Similar results were observed in three independent experiments. (**C**) Immunoblot analysis of AIF in nuclear and mitochondrial fractions of 661W cells treated as in (**A**). PARP1 and COX IV were detected as nuclear or mitochondrial marker, respectively. (**D**, **E**) Relative AIF contents in nuclear (**D**) or mitochondrial (**E**) fractions of the treated cells were determined by the immunoblot intensities in (**C**). $^{*}P < 0.05$ indicates significant differences between cells treated with *at*RAL in mock-medium versus IRBP-medium.

that NOX1 expression (Fig. 4C) and protein *S*-nitrosylation were significantly increased in 661W cells treated with *at*RAL (Fig. 5C). In addition, both *at*RAL (Fig. 1) and NOX1 (Figs. 4E, 4F) were increased in the *Irbp*$^{-/-}$ ocular tissues. Consistent with these results, IRBP inhibited the *at*RAL-mediated NOX1 upregulation and protein *S*-nitrosylation (Figs. 4D, 5E, 5F). Since oxidative and nitrosative stresses are pathologic mechanisms involved in rod and cone photoreceptor degeneration in retinal degenerative diseases,[35,51–53] our results suggest that IRBP plays an important role in protection of photoreceptors from oxidative stress through suppression of *at*RAL accumulation and its thiol-dependent antioxidant activity.[54]

In pathophysiologic conditions, mitochondria are the main producers of ROS; and excessive ROS induces oxidative stress that results in mitochondrial dysfunction in the cells.[47,55] In addition, mitochondrial dysfunction is often associated with activation of various cell death signals. Translocation of AIF from the mitochondrial intermembranous space to the nucleus is one of the important cell death factors that promotes DNA fragmentation and cell death.[37] In the present study, we found that treatment of 661W cells with *at*RAL in the absence of IRBP caused depolarization of mitochondrial membranes (Figs. 6A, 6B), and this mitochondrial damage was accompanied by translocation of AIF into the nuclei of the cells (Figs. 6C, 6D). These results are consistent with previous studies showing that Vitamin A derivative and β-carotene cleavage products, including retinaldehydes, induce cellular oxidative stress and mitochondrial dysfunction.[56,57] Interestingly, it has been shown that IRBP binds carotenoids with a K_D similar to that of retinoids,[41] suggesting that IRBP may inhibit carotenoid cleavage that produces retinaldehydes. The present study and the previous studies also suggest that *at*RAL-induced oxidative stress and mitochondrial dysfunction may contribute to retinal degeneration in *Irbp*$^{-/-}$ mice.

In a previous study,[18] we have shown that dark rearing could not prevent degeneration of photoreceptors in *Irbp*$^{-/-}$ mice. This observation suggests that IRBP has an unidentified function(s) necessary for photoreceptor survival. Expression of IRBP in the developing retina implicates a potential role for IRBP in retinal development and/or maturation.[6,58] Wisard et al.[21] have found that the size and weight of *Irbp*$^{-/-}$ mouse eyes are greater than those of WT mice. The excessive ocular enlargement starts between P7 and P10. Although the mechanism of how IRBP regulates ocular development remains

unknown, it is known that the IPM, where IRBP accumulates, contains numerous growth and neurotrophic factors that regulate cell proliferation, differentiation, and survival.[59,60] The significant increase of TNF in the *Irbp*$^{-/-}$ IPM suggests that IRBP is required for maintaining IPM homeostasis essential for retinal neurodevelopment and function. Both a*t*RAL-mediated cellular damages and aberrant regulation of extracellular signaling proteins in the IPM may contribute to retinal degeneration in *Irbp*$^{-/-}$ mice. Identification of IRBP-interacting protein in the IPM is therefore important for understanding the molecular mechanism of IRBP function and may contribute to the development of therapeutic interventions for retinal dystrophy caused by IRBP mutations.

Acknowledgments

The authors thank Muayyad R. Al-Ubaidi for the 661W cells and Robin J. Jin for editorial assistance.

Supported by Grants from National Institutes of Health (EY021208 to M. J.; GM103340 to LSU Neuroscience COBRE facility), Research to Prevent Blindness and Louisiana Lions Eye Foundation (to LSU Department of Ophthalmology).The authors alone are responsible for the content and writing of the paper.

Disclosure: **M. Lee**, None; **S. Li**, None; **K. Sato**, None; **M. Jin**, None

References

1. Parish CA, Hashimoto M, Nakanishi K, Dillon J, Sparrow J. Isolation and one-step preparation of A2E and iso-A2E, fluorophores from human retinal pigment epithelium. *Proc Natl Acad Sci U S A*. 1998;95:14609–14613.
2. Boyer NP, Higbee D, Currin MB, et al. Lipofuscin and N-retinylidene-N-retinylethanolamine (A2E) accumulate in retinal pigment epithelium in absence of light exposure: their origin is 11-cis-retinal. *J Biol Chem*. 2012;287:22276–22286.
3. Sparrow JR, Fishkin N, Zhou J, et al. A2E, a byproduct of the visual cycle. *Vision Res*. 2003;43:2983–2990.
4. Maeda A, Maeda T, Golczak M, Palczewski K. Retinopathy in mice induced by disrupted all-trans-retinal clearance. *J Biol Chem*. 2008;283:26684–26693.
5. Weng J, Mata NL, Azarian SM, Tzekov RT, Birch DG, Travis GH. Insights into the function of Rim protein in photoreceptors and etiology of Stargardt's disease from the phenotype in abcr knockout mice. *Cell*. 1999;98:13–23.
6. Gonzalez-Fernandez F, Healy JI. Early expression of the gene for interphotoreceptor retinol-binding protein during photoreceptor differentiation suggests a critical role for the interphotoreceptor matrix in retinal development. *J Cell Biol*. 1990;111:2775–2784.
7. Lin ZS, Fong SL, Bridges CD. Retinoids bound to interstitial retinol-binding protein during light and dark-adaptation. *Vision Res*. 1989;29:1699–1709.
8. Adler AJ, Spencer SA. Effect of light on endogenous ligands carried by interphotoreceptor retinoid-binding protein. *Exp Eye Res*. 1991;53:337–346.
9. Crouch RK, Hazard ES, Lind T, Wiggert B, Chader G, Corson DW. Interphotoreceptor retinoid-binding protein and alpha-tocopherol preserve the isomeric and oxidation state of retinol. *Photochem Photobiol*. 1992;56:251–255.
10. Borst DE, Redmond TM, Elser JE, et al. Interphotoreceptor retinoid-binding protein: gene characterization, protein repeat structure, and its evolution. *J Biol Chem*. 1989;264:1115–1123.
11. Gonzalez-Fernandez F. Interphotoreceptor retinoid-binding protein: an old gene for new eyes. *Vision Res*. 2003;43:3021–3036.
12. Carlson A, Bok D. Promotion of the release of 11-cis-retinal from cultured retinal pigment epithelium by interphotoreceptor retinoid-binding protein. *Biochemistry*. 1992;31:9056–9062.
13. Edwards RB, Adler AJ. IRBP enhances removal of 11-cis-retinaldehyde from isolated RPE membranes. *Exp Eye Res*. 2000;70:235–245.
14. Qtaishat NM, Wiggert B, Pepperberg DR. Interphotoreceptor retinoid-binding protein (IRBP) promotes the release of all-trans retinol from the isolated retina following rhodopsin bleaching illumination. *Exp Eye Res*. 2005;81:455–463.
15. Wu Q, Blakeley LR, Cornwall MC, Crouch RK, Wiggert BN, Koutalos Y. Interphotoreceptor retinoid-binding protein is the physiologically relevant carrier that removes retinol from rod photoreceptor outer segments. *Biochemistry*. 2007;46:8669–8679.
16. Betts-Obregon BS, Gonzalez-Fernandez F, Tsin AT. Interphotoreceptor retinoid-binding protein (IRBP) promotes retinol uptake and release by rat Muller cells (rMC-1) in vitro: implications for the cone visual cycle. *Invest Ophthalmol Vis Sci*. 2014;55:6265–6271.
17. Liou GI, Fei Y, Peachey NS, et al. Early onset photoreceptor abnormalities induced by targeted disruption of the interphotoreceptor retinoid-binding protein gene. *J Neurosci*. 1998;18:4511–4520.
18. Jin M, Li S, Nusinowitz S, et al. The role of interphotoreceptor retinoid-binding protein on the translocation of visual retinoids and function of cone photoreceptors. *J Neurosci*. 2009;29:1486–1495.
19. Parker RO, Fan J, Nickerson JM, Liou GI, Crouch RK. Normal cone function requires the interphotoreceptor retinoid binding protein. *J Neurosci*. 2009;29:4616–4621.
20. Kolesnikov AV, Tang PH, Parker RO, Crouch RK, Kefalov VJ. The mammalian cone visual cycle promotes rapid M/L-cone pigment regeneration independently of the interphotoreceptor retinoid-binding protein. *J Neurosci*. 2011;31:7900–7909.
21. Wisard J, Faulkner A, Chrenek MA, et al. Exaggerated eye growth in IRBP-deficient mice in early development. *Invest Ophthalmol Vis Sci*. 2011;52:5804–5811.
22. Arno G, Hull S, Robson AG, et al. Lack of interphotoreceptor retinoid binding protein caused by homozygous mutation of rbp3 is associated with high myopia and retinal dystrophy. *Invest Ophthalmol Vis Sci*. 2015;56:2358–2365.
23. den Hollander AI, McGee TL, Ziviello C, et al. A homozygous missense mutation in the IRBP gene (RBP3) associated with autosomal recessive retinitis pigmentosa. *Invest Ophthalmol Vis Sci*. 2009;50:1864–1872.
24. Li S, Yang Z, Hu J, et al. Secretory defect and cytotoxicity: the potential disease mechanisms for the retinitis pigmentosa (RP)-associated interphotoreceptor retinoid-binding protein (IRBP). *J Biol Chem*. 2013;288:11395–11406.
25. Sato K, Li S, Gordon WC, et al. Receptor interacting protein kinase-mediated necrosis contributes to cone and rod photoreceptor degeneration in the retina lacking interphotoreceptor retinoid-binding protein. *J Neurosci*. 2013;33:17458–17468.
26. Adler AJ, Edwards RB. Human interphotoreceptor matrix contains serum albumin and retinol-binding protein. *Exp Eye Res*. 2000;70:227–234.
27. Li S, Lee J, Zhou Y, et al. Fatty acid transport protein 4 (FATP4) prevents light-induced degeneration of cone and rod photoreceptors by inhibiting RPE65 isomerase. *J Neurosci*. 2013;33:3178–3189.
28. Jin M, Li S, Moghrabi WN, Sun H, Travis GH. Rpe65 is the retinoid isomerase in bovine retinal pigment epithelium. *Cell*. 2005;122:449–459.

29. Jin M, Yuan Q, Li S, Travis GH. Role of LRAT on the retinoid isomerase activity and membrane association of Rpe65. *J Biol Chem*. 2007;282:20915–20924.
30. Tan E, Ding XQ, Saadi A, Agarwal N, Naash MI, Al-Ubaidi MR. Expression of cone-photoreceptor-specific antigens in a cell line derived from retinal tumors in transgenic mice. *Invest Ophthalmol Vis Sci*. 2004;45:764–768.
31. Lee MS, Yoon HD, Kim JI, Choi JS, Byun DS, Kim HR. Dioxinodehydroeckol inhibits melanin synthesis through PI3K/Akt signalling pathway in alpha-melanocyte-stimulating hormone-treated B16F10 cells. *Exp Dermatol*. 2012;21:471–473.
32. Li S, Izumi T, Hu J, et al. Rescue of enzymatic function for disease-associated RPE65 proteins containing various missense mutations in non-active sites. *J Biol Chem*. 2014;289:18943–18956.
33. Black RA, Rauch CT, Kozlosky CJ, et al. A metalloproteinase disintegrin that releases tumour-necrosis factor-alpha from cells. *Nature*. 1997;385:729–733.
34. Shurety W, Merino-Trigo A, Brown D, Hume DA, Stow JL. Localization and post-Golgi trafficking of tumor necrosis factor-alpha in macrophages. *J Interferon Cytokine Res*. 2000;20:427–438.
35. Komeima K, Usui S, Shen J, Rogers BS, Campochiaro PA. Blockade of neuronal nitric oxide synthase reduces cone cell death in a model of retinitis pigmentosa. *Free Radic Biol Med*. 2008;45:905–912.
36. Cano M, Wang L, Wan J, et al. Oxidative stress induces mitochondrial dysfunction and a protective unfolded protein response in RPE cells. *Free Radic Biol Med*. 2014;69:1–14.
37. Susin SA, Lorenzo HK, Zamzami N, et al. Molecular characterization of mitochondrial apoptosis-inducing factor. *Nature*. 1999;397:441–446.
38. Gonzalez-Fernandez F, Betts-Obregon B, Yust B, et al. Interphotoreceptor retinoid-binding protein protects retinoids from photodegradation. *Photochem Photobiol*. 2015;91:371–378.
39. Haeseleer F, Jang GF, Imanishi Y, et al. Dual-substrate specificity short chain retinol dehydrogenases from the vertebrate retina. *J Biol Chem*. 2002;277:45537–45546.
40. Perrault I, Hanein S, Gerber S, et al. Retinal dehydrogenase 12 (RDH12) mutations in leber congenital amaurosis. *Am J Hum Genet*. 2004;75:639–646.
41. Vachali PP, Besch BM, Gonzalez-Fernandez F, Bernstein PS. Carotenoids as possible interphotoreceptor retinoid-binding protein (IRBP) ligands: a surface plasmon resonance (SPR) based study. *Arch Biochem Biophys*. 2013;539:181–186.
42. Gonzalez-Fernandez F, Baer CA, Ghosh D. Module structure of interphotoreceptor retinoid-binding protein (IRBP) may provide bases for its complex role in the visual cycle—structure/function study of Xenopus IRBP. *BMC Biochem*. 2007;8:15.
43. Gonzalez-Fernandez F, Bevilacqua T, Lee KI, et al. Retinol-binding site in interphotoreceptor retinoid-binding protein (IRBP): a novel hydrophobic cavity. *Invest Ophthalmol Vis Sci*. 2009;50:5577–5586.
44. Tezel G, Wax MB. Increased production of tumor necrosis factor-alpha by glial cells exposed to simulated ischemia or elevated hydrostatic pressure induces apoptosis in cocultured retinal ganglion cells. *J Neurosci*. 2000;20:8693–8700.
45. Zhang Q, Steinle JJ. IGFBP-3 inhibits TNF-alpha production and TNFR-2 signaling to protect against retinal endothelial cell apoptosis. *Microvasc Res*. 2014;95:76–81.
46. Mize RR, Lo F. Nitric oxide, impulse activity, and neurotrophins in visual system development(1). *Brain Res*. 2000;886:15–32.
47. Tezel G. Oxidative stress in glaucomatous neurodegeneration: mechanisms and consequences. *Prog Retin Eye Res*. 2006;25:490–513.
48. Pietri M, Schneider B, Mouillet-Richard S, et al. Reactive oxygen species-dependent TNF-alpha converting enzyme activation through stimulation of 5-HT2B and alpha1D autoreceptors in neuronal cells. *FASEB J*. 2005;19:1078–1087.
49. Zhang Z, Kolls JK, Oliver P, et al. Activation of tumor necrosis factor-alpha-converting enzyme-mediated ectodomain shedding by nitric oxide. *J Biol Chem*. 2000;275:15839–15844.
50. Haruta M, Bush RA, Kjellstrom S, et al. Depleting Rac1 in mouse rod photoreceptors protects them from photo-oxidative stress without affecting their structure or function. *Proc Natl Acad Sci U S A*. 2009;106:9397–9402.
51. Shen J, Yang X, Dong A, et al. Oxidative damage is a potential cause of cone cell death in retinitis pigmentosa. *J Cell Physiol*. 2005;203:457–464.
52. Cingolani C, Rogers B, Lu L, Kachi S, Shen J, Campochiaro PA. Retinal degeneration from oxidative damage. *Free Radic Biol Med*. 2006;40:660–669.
53. Komeima K, Rogers BS, Lu L, Campochiaro PA. Antioxidants reduce cone cell death in a model of retinitis pigmentosa. *Proc Natl Acad Sci U S A*. 2006;103:11300–11305.
54. Gonzalez-Fernandez F, Sung D, Haswell KM, Tsin A, Ghosh D. Thiol-dependent antioxidant activity of interphotoreceptor retinoid-binding protein. *Exp Eye Res*. 2014;120:167–174.
55. Usui S, Oveson BC, Iwase T, et al. Overexpression of SOD in retina: need for increase in H2O2-detoxifying enzyme in same cellular compartment. *Free Radic Biol Med*. 2011;51:1347–1354.
56. Murata M, Kawanishi S. Oxidative DNA damage by vitamin A and its derivative via superoxide generation. *J Biol Chem*. 2000;275:2003–2008.
57. Siems W, Sommerburg O, Schild L, Augustin W, Langhans CD, Wiswedel I. Beta-carotene cleavage products induce oxidative stress in vitro by impairing mitochondrial respiration. *FASEB J*. 2002;16:1289–1291.
58. Eisenfeld AJ, Bunt-Milam AH, Saari JC. Immunocytochemical localization of interphotoreceptor retinoid-binding protein in developing normal and RCS rat retinas. *Invest Ophthalmol Vis Sci*. 1985;26:775–778.
59. Hageman GS, Kirchoff-Rempe MA, Lewis GP, Fisher SK, Anderson DH. Sequestration of basic fibroblast growth factor in the primate retinal interphotoreceptor matrix. *Proc Natl Acad Sci U S A*. 1991;88:6706–6710.
60. Tombran-Tink J, Li A, Johnson MA, Johnson LV, Chader GJ. Neurotrophic activity of interphotoreceptor matrix on human Y79 retinoblastoma cells. *J Comp Neurol*. 1992;317:175–186.

Investigative Ophthalmology & Visual Science